Dalton Transactions

PAPER

View Article Online
View Journal | View Issue

Cite this: *Dalton Trans.*, 2019, **48**, 1814

Building *trans*-philicity (*trans*-effect/*trans*-influence) ladders for octahedral complexes by using an NMR probe†

A. C. Tsipis

Received 17th November 2018,
Accepted 2nd January 2019

DOI: 10.1039/c8dt04562c

rsc.li/dalton

NMR *trans*-philicity (*trans*-effect/*trans*-influence) ladders have been built for a broad series of octahedral $[Cr(CO)_5L]^{-/0/+}$ complexes (50 ligands used) by using a ^{13}C NMR probe and quantified through calculation of the $\Delta\sigma = \sigma_{Cr(CO)_5L} - \sigma_{Cr(CO)_5}$ NMR parameter employing DFT computational methods. This quantification notably retrieves the experimental *trans*-orienting series. The excellent linear correlations between the calculated $\Delta\sigma$ NMR parameter and well established ligand electronic parameters, such as the ligand constant P_L and the ligand electrochemical parameter $E_L(L)$, that measure the ligand bonding effects in coordination and organometallic chemistry prompt us to introduce the *trans*-philicity concept as a unified term to cover both the kinetic *trans*-effect and its thermodynamic (ground state) *trans*-influence cousin. The *trans*-philicity for ligand L is defined as the strength of philicity of the coordination site in *trans*-position to itself. *trans*-Effect and *trans*-influence ladders have also been built for the octahedral $[Cr(CO)_5L]^{-/0/+}$ complexes based on the calculated intrinsic bond dissociation energy of the $Cr-CO_{trans}$ bond, IBDE($Cr-CO_{trans}$) to account for the *trans*-effect and the $\nu(C{\equiv}O_{trans})$ and $\nu(Cr-CO_{trans})$ vibrational frequencies, and $R(Cr-CO_{trans})$ bond lengths to develop the *trans*-influence series and compared with the NMR *trans*-philicity ladder.

Introduction

The term '*trans*-influence', being a long-established concept of broad relevance in the realm of inorganic chemistry, was defined first in 1966 by Pidcock *et al.*[1] as the ability of ligand L in a complex to weaken the metal–ligand bond *trans* to itself. This ground-state phenomenon should be distinguished from the kinetic phenomenon called the '*trans*-effect', which is the effect of coordinated ligand L upon the rate of substitution reactions of the ligand in *trans*-position to L.[2,3]

In the mid-1970s, Pickett and Pletcher[4] introduced the electronic ligand parameter P_L defined as $P_L = E_{1/2}[Cr(CO)_6] - E_{1/2}[Cr(CO)_5L]$, which provides a measure of the ligand bonding effects in coordination and organometallic chemistry.[5–10] At the same time Tolman reported the so-called Tolman's electronic parameter (TEP) for phosphanes, R_3P, based on the position of the A_1 $\nu(CO)$ vibration of $(R_3P)Ni(CO)_3$ in the IR spectrum.[11] Later Lever[8,9] reported electronic ligand parameters, $E_L(L)$, for a wide variety of ligands L based on the electrochemical E_0 value for various Ru(III)/Ru(II) redox couples. Perrin *et al.*[12] calculated the predicted A_1 $\nu(CO)$ vibration of $Ni(CO)_3L$ complexes for a wide variety of L (68 ligands) providing a computationally derived ligand electronic parameter (CEP). Zobi[13] carried out a density functional theory (DFT) and natural population analysis (NPA) of octahedral *fac*-$[M(CO)_3L_3]_n$ (M = Re, Ru, and Mn), square-planar *cis*-$[Pt(CO)_2L_2]_n$, and tetrahedral $[Ni(CO)_3L]_n$ carbonyl complexes in order to understand what effects are probed in these species by IR spectroscopy and electrochemistry as a function of the ligand electronic parameter of the associated L. Very recently Cremer and Kraka[14] introduced the metal–ligand electronic parameter (MLEP) based on the local stretching force constant of the M–L bond.

In 2000 Coe and Glenwright[3] presented an extensive survey of the occurrences and origins of both structural *trans*-effects (STEs) and kinetic *trans*-effects (KTEs) in octahedral complexes. From the analysis of a great deal of crystallographic data, the authors attempted to propose a universal STE series for ligands in octahedral complexes. Investigations of the *trans*-influence in octahedral complexes have employed a variety of physicochemical techniques, including IR and NMR spectroscopic measurements.[15–17] Wovkulich and Atwood[18] investigated the reactions of *trans*-$Cr(CO)_4LL'$ (L,L' = PBu_3, $P(OMe)_3$, $P(OPh)_3$, PPh_3, $AsPh_3$) to determine the effect of a *trans*-orientation of ligands. Interestingly, neither σ nor π nor

Laboratory of Inorganic and General Chemistry, University of Ioannina, 45110 Ioannina, Greece. E-mail: attsipis@uoi.gr

†Electronic supplementary information (ESI) available: Charts S1 and S2, Fig. S1–S6, and Tables S1–S8. See DOI: 10.1039/c8dt04562c

the ratio of σ-to-π bonding correlates well with the observed rates. However, for a given dissociating ligand from the *trans*-$Cr(CO)_4LL'$ complexes, an extremely good correlation between the rate and the ν(CO) stretching frequency was obtained. A systematic compilation of structural data from the CSD provided a quantification of the *trans*-influence for the ligands O = CX_2, NR_3, pyridine, Cl^-, S = CX_2, SR_2, PPh_3, CO, η^2-C≡C, $C_6F_5^-$, Ph^-, CR_3^-, and H^-, at least as they effect the metal–ligand bonding to the probe ligands Cl^- and PPh_3 in square-planar d^8 and octahedral d^6 (low-spin) complexes.[19] Recently Guégan *et al.*[20] characterized and rationalized the *trans*-effects in octahedral complexes by theoretical approaches using tools from conceptual DFT, namely the Dual Descriptor (DD)[21–23] and the Extended Transition State-Natural Orbitals for Chemical Valence[24–26] (ETS-NOCV) and drew a quantitative scale of the *trans*-orienting ligands.

Considering the high sensitivity of the ^{13}C NMR isotropic shielding tensor elements to small structural/electronic changes and the electronic nature of *trans*-philicity, which provides a measure of the ligand bonding effects in coordination and organometallic chemistry, we thought it would be advisable to assess the performance of the ^{13}C NMR isotropic shielding tensor elements in building a reliable *trans*-philicity ladder for octahedral $[Cr(CO)_5L]^{-/0/+}$ complexes with a wide variety of ligands (50 ligands) commonly used in coordination and organometallic chemistry. The use of the unified *trans*-philicity concept expressed by the ^{13}C NMR descriptor avoids confusion in the ambiguous use of both the kinetic and equilibrium phenomena. Moreover *trans*-effect and *trans*-influence ladders have also been built for the octahedral $[Cr(CO)_5L]^{-/0/+}$ complexes based on the calculated intrinsic bond dissociation energy of the Cr–CO_{trans} bond, IBDE(Cr–CO_{trans}), to develop the *trans*-effect series and the ν(C≡O_{trans}) and ν(Cr–CO_{trans}) vibrational frequencies, and R(Cr–CO_{trans}) bond lengths to develop the *trans*-influence series and compared them with the NMR *trans*-philicity ladder.

Results and discussion

Computational details

All calculations were performed using the Gaussian 09, version D.01 program suite.[27] The geometries of the complexes were fully optimized, without symmetry constraints, employing the 1999 hybrid functional of Perdew, Burke, and Ernzerhof[28–30] as implemented in the Gaussian09, version D.01 program suite. This functional uses 25% exchange and 75% correlation weighting and is denoted as PBE0. Geometry optimization of the octahedral $[Cr(CO)_5L]^{-/0/+}$ complexes was done in solution (CH_2Cl_2 solvent) using the Def2-TZVP basis set[31] for Cr and the 6-31G(d,p) for all main group elements (E). Solvent effects were accounted for by means of the Polarizable Continuum Model (PCM) using the integral equation formalism variant (IEF-PCM) being the default self-consistent reaction field (SCRF) method.[32] Hereafter the computational protocol used in DFT calculations of $[Cr(CO)_5L]^{-/0/+}$ complexes is abbreviated as PBE0/Def2-TZVP(Cr)∪6-31G(d,p)(E)/PCM. However, to ensure that computed isotropic σ ^{13}C shielding tensor elements are reliable, they have also been calculated by the PBE0/Def2-TZVP(Cr)∪6-311++G(d,p)(E)/PCM computational protocol using the more sophisticated 6-311++G(d,p)(E) basis set for all main group elements. All stationary points have been identified as minima (number of imaginary frequencies NImag = 0). NBO population analysis was performed using Weinhold's methodology.[33,34] Magnetic shielding tensors have been computed with the gauge-including atomic orbital DFT method,[35,36] as implemented in the Gaussian09 series of programs.

Building the *trans*-philicity ladder

The isotropic σ ^{13}C shielding tensor elements and R(Cr–CO_{trans}) bond lengths of octahedral $[Cr(CO)_5L]^{-/0/+}$ complexes calculated by the PBE0/Def2-TZVP(Cr)∪6-31G(d,p)(E)/PCM and PBE0/Def2-TZVP(Cr)∪6-311++G(d,p)(E)/PCM computational protocols in dichloromethane solution, along with the well established ligand electronic parameters P_L and E_L(L) are given in the ESI (Table S1†). To the best of our knowledge experimental data for δ ^{13}C NMR chemical shifts of $[Cr(CO)_5L]^{-/0/+}$ complexes are available only for the $Cr(CO)_6$ complex and the "free" CO ligand, which are 212 and 184.4 ppm respectively.[37] Therefore we assessed the performance of the PBE0/Def2-TZVP(Cr)∪6-31G(d,p)(E)/PCM and PBE0/Def2-TZVP(Cr)∪6-311++G(d,p)(E)/PCM computational protocols in the calculation of the ^{13}C NMR spectra of $[Cr(CO)_5L]^{-/0/+}$ complexes using this insufficient benchmark. Calculations of δ ^{13}C NMR chemical shifts of the $Cr(CO)_6$ complex and the "free" CO ligand employing the PBE0/Def2-TZVP(Cr)∪6-31G(d,p)(E)/PCM and (PBE0/Def2-TZVP(Cr)∪6-311++G(d,p)(E)/PCM) computational protocols predicted δ ^{13}C NMR chemical shifts of 210.2 (226.8) and 186.1 (197.6) ppm respectively. Noteworthily, the GIAO/PBE0/Def2-TZVP(Cr)∪6-31G(d,p)(E)/PCM computational protocol is a better performer in the calculation of the ^{13}C NMR spectra of $[Cr(CO)_5L]^{-/0/+}$ complexes than the PBE0/Def2-TZVP(Cr)∪6-311++G(d,p)(E)/PCM one. To test further whether the established trends hold up independent of the computational protocol, the $\Delta\sigma$ ^{13}C NMR descriptors of *trans*-philicity for the $[Cr(CO)_5L]^{-/0/+}$ complexes were calculated employing the PBE0/Def2-TZVP(Cr)∪6-31G(d,p)(E)/PCM and the more sophisticated PBE0/Def2-TZVP(Cr)∪6-311++G(d,p)(E)/PCM computational protocols (Table 1).

It can be seen that the NMR *trans*-philicity ladders constructed by the two computational protocols are similar with some minor local reversed orders in the *trans*-philicity series of similar ligands. The PBE0/Def2-TZVP(Cr)∪6-31G(d,p)(E)/PCM computational protocol predicts for the NCR ligands the order: NCH > NCPh > NCMe, while the PBE0/Def2-TZVP(Cr)∪6-311++G(d,p)(E)/PCM computational protocol predicts the order: NCMe > NCPh > NCH. Consideration of the σ-donor and π-acceptor abilities of the NCR ligands supports the order predicted by the PBE0/Def2-TZVP(Cr)∪6-31G(d,p)(E)/PCM computational protocol. Similarly, for the strong σ-donor ligands, Ph^-, H^-, *t*-Bu^- and Me^-, the PBE0/Def2-TZVP(Cr)∪6-31G(d,p)

Table 1 The $\Delta\sigma$ ^{13}C descriptor of *trans*-philicity for octahedral $[Cr(CO)_5L]^{-/0/+}$ complexes calculated by the PBE0/Def2-TZVP(Cr)∪6-31G(d,p)(E)/PCM and PBE0/Def2-TZVP(Cr)∪6-311++G(d,p)(E)/PCM computational protocols

	$\Delta\sigma$ ^{13}C (ppm)			$\Delta\sigma$ ^{13}C (ppm)	
Ligand	6-31G (d,p)	6-311++G (d,p)	Ligand	6-31G (d,p)	6-311++G (d,p)
N^+	53.87	62.29	OCN^-	13.08	13.42
NO^+	41.40	45.42	H_2O	13.07	13.88
CO	21.12	25.61	H_2S	13.01	15.33
F^-	20.87	**17.26**	N_3^-	12.93	14.30
N_2	18.56	21.33	CH_2FCOO^-	12.85	13.45
CNH	18.45	22.14	CH_3COO^-	12.82	13.60
PF_3	18.36	22.38	$HCOO^-$	12.77	13.56
OH^-	18.05	**17.14**	$C_6H_5COO^-$	12.73	13.63
CNPh	17.70	21.04	$CHCl_2COO^-$	12.72	13.52
CNMe	17.43	20.97	CH_2BrCOO^-	12.71	13.60
NCH	16.79	18.24	$CH_3(CH_2)_2COO^-$	12.61	13.47
BrO^-	16.75	16.80	CH_2ClCOO^-	12.59	13.51
NCS^-	16.33	**42.61**	$CH_3CH_2COO^-$	12.55	13.42
ClO^-	16.33	16.45	CCl_3COO^-	12.54	13.44
NCPh	16.30	18.50	NH_2^-	11.88	13.31
NCMe	16.24	18.52	NO_3^-	11.77	**27.77**
NH_3	15.32	17.21	Cl^-	10.50	11.82
CN^-	14.67	17.06	SCN^-	10.36	11.80
Carbene	14.51	16.88	Br^-	9.39	10.11
Py	14.44	15.92	SH^-	9.35	10.73
PH_3	14.40	17.02	Ph^-	9.18	10.01
PMe_3	13.78	15.73	$SnCl_3^-$	9.17	10.24
FO^-	13.76	13.32	H^-	8.24	8.62
PPh_3	13.75	15.55	*t*-Bu^-	7.83	8.36
NO_2^-	13.56	14.40	Me^-	7.29	8.42

(E)/PCM computational protocol predicts the order: $Ph^- > H^- > t\text{-}Bu^- > Me^-$, while the PBE0/Def2-TZVP(Cr)∪6-311++G(d,p)(E)/PCM computational protocol predicts the order: $Ph^- > H^- > Me^- > t\text{-}Bu^-$. In the latter series Me^- exerts a stronger *trans*-effect than *t*-Bu^-, which is in contrast to the experimentally established *trans*-effect series.[15] Unexpectedly, in the *trans*-philicity ladder constructed by the PBE0/Def2-TZVP(Cr)∪6-311++G(d,p)(E)/PCM computational protocol four ligands, namely F^-, OH^-, NCS^- and NO_3^- (marked in bold in Table 1), are not placed in the right rungs of the ladder. This is due to the fact that the PBE0/Def2-TZVP(Cr)∪6-311++G(d,p)(E)/PCM computational protocol predicts lower $\Delta\sigma$ ^{13}C values for the F^- and OH^- ligands by 3.61 and 0.91 ppm respectively and higher by 16.00 ppm and 26.28 ppm for the NO_3^- and NCS^- ligands. According to these values the NO_3^- and NCS^- ligands exhibit very strong *trans*-philicity (*trans*-effect/*trans*-influence), which is not the case for the experimentally established *trans*-effect series,[15] where the NO_3^- and NCS^- ligands exhibit a very weak and moderate *trans*-effect. Generally, the $\Delta\sigma$ ^{13}C descriptors calculated by the PBE0/Def2-TZVP(Cr)∪6-311++G(d,p)(E)/PCM computational protocol are higher by 0.05–8.42 ppm (weighted average 1.61 ppm) than the $\Delta\sigma$ ^{13}C calculated by the PBE0/Def2-TZVP(Cr)∪6-31G(d,p)(E)/PCM one (Table 1). Therefore herein we will present and analyze only the more realistic results obtained by the GIAO/PBE0/Def2-TZVP(Cr)∪6-31G(d,p)(E)/PCM computational protocol and the analogous results obtained by the PBE0/Def2-TZVP(Cr)∪6-311++G(d,p)(E)/PCM computational protocol will be given in the ESI.†

Chart 1 shows the *trans*-philicity ladder constructed by the calculated $\Delta\sigma = \sigma_{Cr(CO)_5L} - \sigma_{Cr(CO)_5}$ NMR parameter and compared with the *trans*-effect ladder quantified by the intrinsic bond dissociation energy of the Cr–CO_{trans} bond, and the IBDE (Cr–CO_{trans}) probe[14] and with the *trans*-influence ladder quantified by the ν(C≡O_{trans}) probe. *trans*-Influence ladders probed by the R(Cr–CO_{trans}) and ν(Cr–CO_{trans}) descriptors are given in Chart 2, while the ν(Cr–CO_{trans}) and ν(C≡O_{trans}) stretching vibrational frequencies calculated by the PBE0/Def2-TZVP(Cr)∪6-31G(d,p)(E)/PCM and PBE0/Def2-TZVP(Cr)∪6-311++G(d,p)(E)/PCM computational protocols are given in the ESI (Tables S2†). The analogous *trans*-philicity, *trans*-effect and *trans*-influence ladders constructed by the PBE0/Def2-TZVP(Cr)∪6-311++G(d,p)(E)/PCM computational protocol are given in the ESI (Charts S1 and S2†).

To the best of our knowledge, there have been no extensive *trans*-influence and *trans*-effect series studied for octahedral complexes for comparisons to be made with the *trans*-philicity ladder. The quantitative computational *trans*-effect scale provided by Guégan *et al.*[20] was limited to very few ligands, namely CH_3^-, CO, NO_2^-, pyridine, NH_3, Cl^- and H_2O. The authors showed that the grand-canonical dual descriptor referred to as the DD descriptor partitioned into reactive domains can be used to draw quantitative scales of the *trans*-orienting ligands in octahedral $[Rh(NH_3)_4(H_2O)X]^{n+}$ and $[Ru(NH_3)_5X]^{n+}$ complexes. On the basis of the $\Delta s(D_M^+)$ descriptors the following trends for the X ligands are obtained:

$$NO_2^- < CH_3^- \approx CO < NH_3 < Cl^- < Py < H_2O$$

$$NO_2^- < CH_3^- \approx CO < Py < Cl^- < H_2O$$

for Rh complexes and Ru complexes respectively with the NO_2^-, CH_3^- and CO ligands being strong *trans*-orienting ligands in both cases.

A general kinetic *trans*-effect (KTE) sequence for octahedral complexes has been established as follows:[38]

$$H_2O < OH^- < NH_3 <\approx RNH_2 < Py < Cl^- < Br^- < I^- \approx SCN^- \approx NO_2^- < SO_3H^- < PR_3 \approx SR_2 \approx tu \approx Me^- < NO \approx \eta^2 - C_2H_4 \approx CO \approx CN^-$$

On the other hand, for square planar platinum(II) complexes the *trans*-effect order is:[15]

$$H_2O \approx NO_3^- < OH^- < NH_3 < Cl^- < Br^- < I^- \approx SCN^- \approx NO_2^- \approx PR_3 \ll CO \approx C_2H_4 \approx CN^- \approx CH_3^- \approx H^-$$

Noteworthily, the *trans*-philicity, *trans*-effect and *trans*-influence series quantified by the $\Delta\sigma$ ^{13}C NMR, IBDE(Cr–CO_{trans}) and ν(C≡O_{trans}) probes roughly retrieves the experimentally established *trans*-effect series.

Charts 1 and 2 show that the *trans*-philicity ladder goes roughly parallel to the *trans*-effect and *trans*-influence ladders. Indeed all ladders are almost similar with some minor deviations due to the different probes used to quantify *trans*-phili-

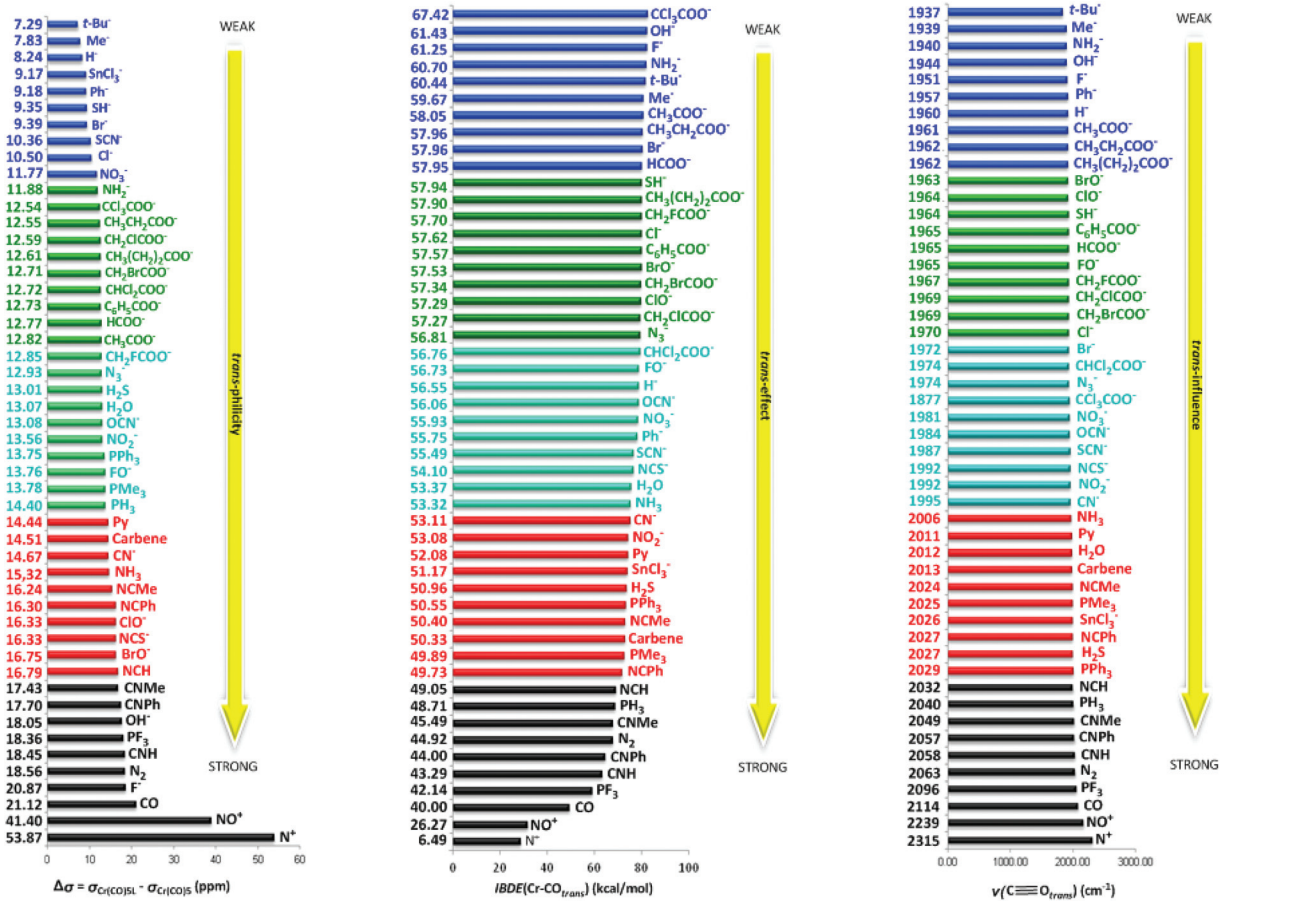

Chart 1 *trans*-Philicity, *trans*-effect and *trans*-influence ladders for octahedral $[Cr(CO)_5L]^{-/0/+}$ complexes quantified by $\Delta\sigma$ ^{13}C NMR, intrinsic bond dissociation energy of the Cr–CO_{trans} bond, IBDE(Cr–CO_{trans}) and the stretching vibrational frequency and $\nu(C{\equiv}O_{trans})$ probes respectively.

city, *trans*-effect and *trans*-influence. Perusal of the NMR *trans*-philicity, kinetic *trans*-effect and ground state *trans*-influence ladders reveals that NMR is the more sensitive probe in the quantification of *trans*-philicity than the IBDE(Cr–CO_{trans}), $\nu(C{\equiv}O_{trans})$, ν(Cr–CO_{trans}) and R(Cr–CO_{trans}) probes used to quantify the *trans*-effect and *trans*-influence.

Inspection of the *trans*-philicity, *trans*-effect and *trans*-influence ladders reveals that the strongest *trans*-philicity, *trans*-effect and *trans*-influence is exhibited by the strong π-acceptor ligands (for example N^+, NO^+, CO and isonitriles) and the weakest one by the strong σ-donor ligands (for example Me^-, *t*-Bu^-, H^-, Ph^-, SH^-, halides and NH_2^-). Other commonly used ligands in coordination and organometallic chemistry, such as carbenes, pyridine, NH_3, nitriles and phosphanes, exhibit moderate *trans*-philicity, *trans*-effect and *trans*-influence in line with the established KTE sequence.[15] Depending on the probe used to quantify *trans*-philicity, *trans*-effect and *trans*-influence some minor changes in the trends of these ligands along the series are observed. For example the strong σ-donor OH^- and F^- ligands exert strong *trans*-philicity, but weak *trans*-effect and *trans*-influence. The strong σ-donor OH^- and F^- ligands induce charge transfer towards the Cr central atom, thus increasing the electron density on Cr to enhance the Cr–CO_{trans} back donation. Therefore the $\nu(C{\equiv}O)$ stretching frequency decreases and the Cr–CO_{trans} bond dissociation energy increases.

The σ-donor/π-acceptor cyanide (CN^-) ligand is placed in the region of moderate instead of strong *trans*-philicity, *trans*-effect and *trans*-influence. This could be due to anisotropic effects from ligands containing unsaturated groups or aromatic rings on the calculated ^{13}C NMR shielding tensor elements.

It is important to be noted that the set of carboxylato ligands studied exhibit almost similar weak *trans*-philicity, *trans*-effect and *trans*-influence. The estimated $\Delta\sigma$ ^{13}C NMR values for the carboxylato complexes range from 12.54 up to 12.94 ppm. Note that the $\Delta\sigma$ ^{13}C values calculated by the PBE0/Def2-TZVP(Cr)∪6-311++G(d,p)(E)/PCM computational protocol range from 13.44 to 13.63 ppm. Generally the isotropic σ_{calcd} ^{13}C shielding tensor elements of the $[Cr(CO)_5(RCOO)]^-$ complexes seems to be less sensitive to the pK_a of carboxylic acids which is related to the nucleophilicity of the carboxylato ligands.

In order to scrutinize the underlying principles and the origin of *trans*-philicity and throw some light on the still intriguing physics of the *trans*-effect we investigated relationships

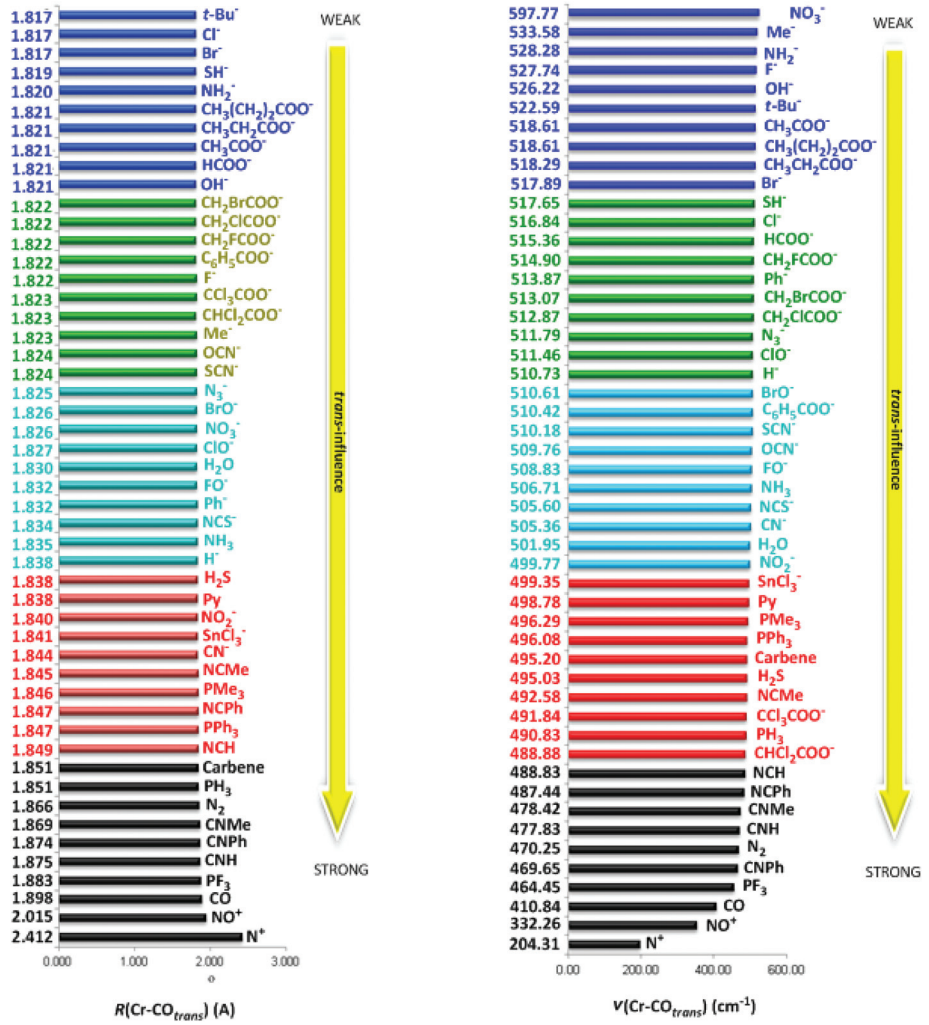

Chart 2 *trans*-Influence ladders for octahedral $[Cr(CO)_5L]^{-/0/+}$ complexes quantified by the $R(Cr{-}CO_{trans})$ bond lengths and $\nu(Cr{-}CO_{trans})$ vibrational frequencies.

between the isotropic σ ^{13}C shielding tensor elements and the well established ligand electronic parameters P_L and $E_L(L)$ and other popular electronic/structural descriptors related to the L–Cr–CO_{trans} bonding. Fig. 1 shows good linear relationships between σ_{calcd} ^{13}C shielding tensor elements and the P_L and $E_L(L)$ parameters. Analogous linear relationships between σ_{calcd} ^{13}C shielding tensor elements calculated by the PBE0/Def2-TZVP(Cr)∪6-311++G(d,p)(E)/PCM computational protocol and the P_L and $E_L(L)$ parameters are shown in the ESI (Fig. S1†). Excellent linear correlations of σ_{calcd} ^{13}C shielding tensor elements with the computationally derived electronic parameter (CEP) and the experimentally derived Tolman electronic parameter (TEP) are also given in the ESI (Fig. S2†).

Fig. 1 shows on the right part that good linear relationships (almost parallel lines) are obtained for two different subsets of ligands L. The first subset consists of 15 ligands, namely CO, N_2, PF_3, NCH, NCPh, NCMe, CNPh, CNMe, NHC(carbene), NCS^-, CN^-, NH_3, N_3^-, OCN^- and $HCOO^-$ that exert moderate to strong *trans*-philicity. The linear relationships σ_{calcd} ^{13}C *vs.* P_L and σ_{calcd} ^{13}C *vs.* $E_L(L)$ parameters for the first subset are shown in red. All ligands of the first subset (except for NH_3) belong to the class of σ-donor/π-acceptor ligands. It should be noted that carbenes are comparatively good σ donor ligands but compared to CO, these ligands are weaker π-acceptors.[39] Noteworthily, the first subset of L consists of ligands bearing unsaturated bonds or aromatic rings that induce anisotropic effects on the calculated σ ^{13}C shielding tensor elements estimated to deshield the ^{13}C nucleus by an average of 3.0 ppm. The second subset consists of 15 ligands, namely PH_3, PMe_3, PPh_3, py, H_2O, H_2S, NO_3^-, NO_2^-, Br^-, Cl^-, SH^-, Me^-, *t*-Bu^- and Ph^-, which exhibit moderate to weak *trans*-philicity. The linear relationships σ_{calcd} ^{13}C *vs.* P_L and σ_{calcd} ^{13}C *vs.* $E_L(L)$ parameters are shown in blue. All ligands of the second subset belong to the classes of σ-donor/π-donor and strong σ-donor ligands. A subset of 5 ligands (N^+, NO^+, F^-, H^- and OH^-) for which P_L and $E_L(L)$ parameters are available are outliers in the σ_{calcd} ^{13}C *vs.* P_L and σ_{calcd} ^{13}C *vs.* $E_L(L)$ parameter relationships. These ligands are strong π-acceptor ligands (N^+, NO^+) and weak

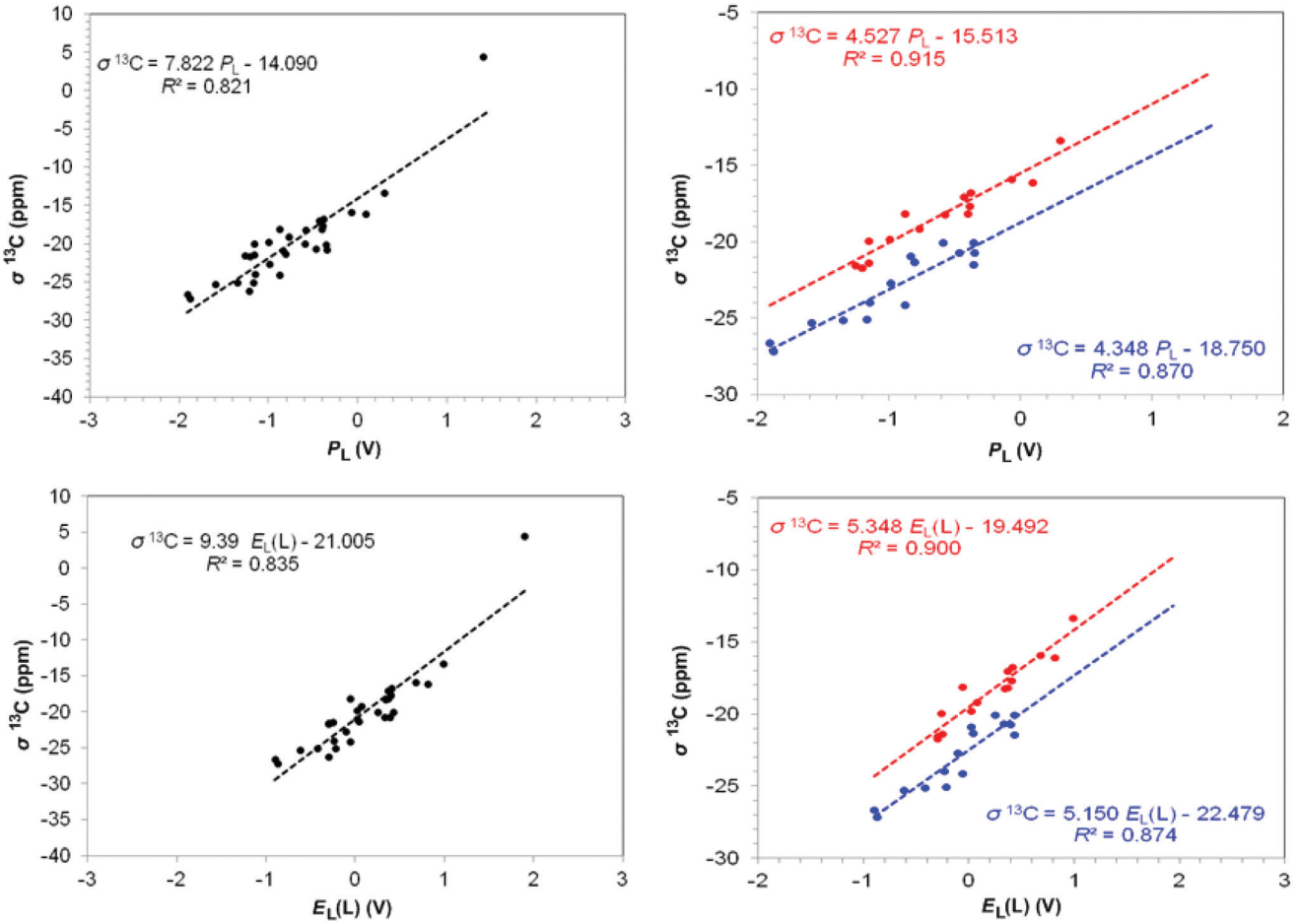

Fig. 1 Linear relationships between σ_{calcd} ^{13}C shielding tensor elements of octahedral $[Cr(CO)_5L]^{-/0/+}$ complexes calculated by the GIAO/PBE0/Def2-TZVP(Cr)∪6-31G(d,p)(E)/PCM computational protocol and the P_L and E_L(L) ligand electronic parameters.

π-donor (F^- and OH^-) ligands. The deviations observed for the outliers could be due either to wrong P_L and E_L(L) parameters or to solvation and hydrogen bond effects on the σ_{calcd} ^{13}C shielding tensor elements.

Considering that ligand substitution reactions in octahedral complexes generally follow a dissociative mechanism the *trans*-effect and *trans*-influence often correlate. Thus the highly *trans*-influencing ligands show a high *trans*-effect. It is obvious then why the *trans*-philicity sequences for the following ligand families retrieves the experimental *trans*-orienting series:

$$Ph^- > H^- > t\text{-}Bu^- > Me^-$$

$$PF_3 > PH_3 > PMe_3 > PPh_3$$

The *trans*-philicity of the halide and hypohalite ligands follows the expected orders:

$$F^- > Cl^- > Br^-$$

$$BrO^- > ClO^- > FO^-$$

Comparison of the NMR *trans*-philicity order (Chart 1) with the *trans*-influence order probed by the R(Cr–CO_{trans}) and ν(Cr–CO_{trans}) descriptors (Chart 2) reveals that strong σ donor ligands exhibit weak *trans*-philicity and *trans*-influence, except for the hydride H^- strong σ donor that exhibits moderate to strong *trans*-influence. The strong π-acceptor ligands ($SnCl_3^-$, N^+, CH^+, NO^+, CO and isonitriles) exert the strongest *trans*-philicity and *trans*-influence, while weak π-acceptor ligands, such as phosphanes, nitriles, NH_3, H_2O, hypohalites and carboxylates, exert moderate to weak *trans*-philicity and *trans*-influence for all probes used. Noteworthily, the σ_{calcd} ^{13}C and ν(C≡O_{trans}) probes are more sensitive to *trans*-philicity and *trans*-influence respectively than the R(Cr–CO_{trans}) and ν(Cr–CO_{trans}) probes. It should be noted that similar trends hold up when employing the PBE0/Def2-TZVP(Cr)∪6-311++G(d,p)(E)/PCM computational protocol (compare Chart S1 with Chart S2†).

Excellent linear correlations between the estimated σ_{calcd} ^{13}C shielding tensor elements and the R(Cr–CO_{trans}), ν(Cr–CO_{trans}), ν(C≡O_{trans}) and IBDE(Cr–CO_{trans}) probes (Fig. 2) reveal that calculated NMR parameters for L are powerful descriptors to quantify the *trans*-philicity of ligands in octahedral $[Cr(CO)_5L]^{-/0/+}$ complexes and demonstrate the proposed establishment of the unified *trans*-philicity concept to cover both *trans*-influence and *trans*-effect. The *trans*-philicity

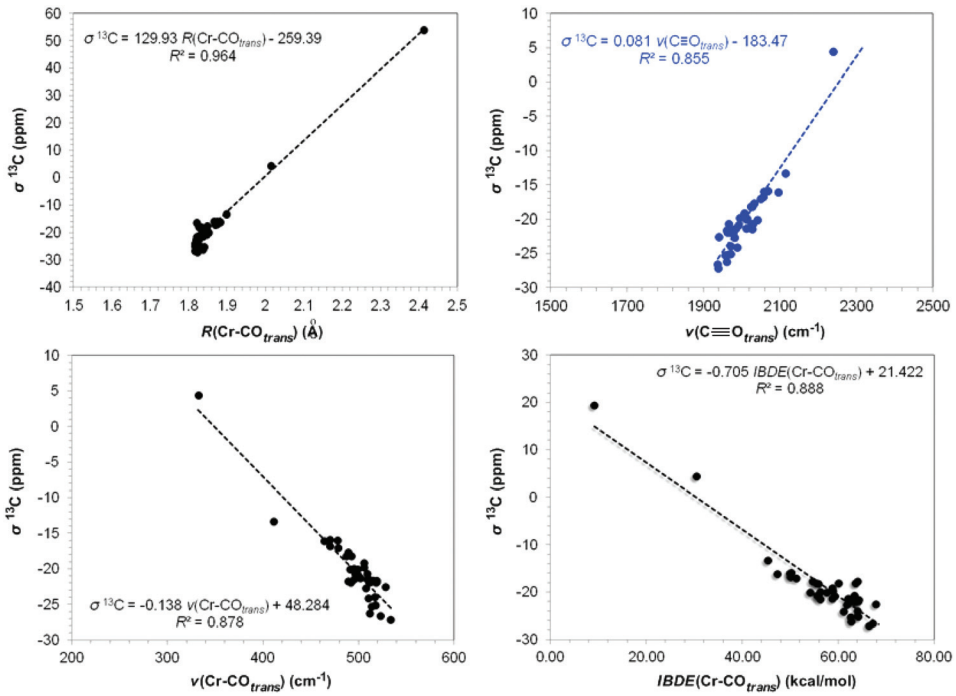

Fig. 2 Linear relationships between σ_{calcd} ^{13}C shielding tensor elements of octahedral $[Cr(CO)_5L]^{-/0/+}$ complexes calculated by the GIAO/PBE0/Def2-TZVP(Cr)∪6-31G(d,p)(E)/PCM computational protocol and the R(Cr–CO$_{trans}$), ν(C≡O$_{trans}$), ν(Cr–CO$_{trans}$) and IBDE(Cr–CO$_{trans}$) descriptors of *trans*-influence of L.

for ligand L is defined as the strength of philicity of the coordination site in *trans*-position to itself. In this respect the use of the unified *trans*-philicity concept expressed by the $\Delta\sigma$ ^{13}C NMR descriptor avoids confusion in the ambiguous use of both the *trans*-effect and *trans*-influence concepts.

If we take into consideration that the primary determinant of *trans*-philicity is likely to be covalent contributions to bonding, whether they arise from σ-donation or π-back-donation, in the formation of the L → Cr dative bond, the electron density is transferred towards the coordination site *trans* to L. Pinter *et al.*[40] showed that during this density accumulation in the *trans*-position, a ligand in this position will be exposed to a Pauli-type repulsion, hence increasing σ-donation results in a stronger repulsion in the *trans*-position, which induces the elongation and labilization of the metal–ligand bond (the Cr–CO$_{trans}$ bond in our case). In this context we searched for correlations between the σ_{calcd} ^{13}C shielding tensor elements of the C≡O ligand and some popular electronic descriptors (such as bond orders, natural atomic charges on the bonded atoms, the $s^xp^yd^z$ character of the σ(Cr–CO$_{trans}$) bonding mode and the occupancy of σ(Cr–CO$_{trans}$) and σ*(Cr–CO$_{trans}$) NBOs) in $[Cr(CO)_5L]^{-/0/+}$ complexes. The isotropic σ_{calcd} ^{13}C shielding tensor elements along with the aforementioned electronic descriptors calculated by the PBE0/Def2-TZVP(Cr)∪6-31G(d,p)(E)/PCM and PBE0/Def2-TZVP(Cr)∪6-311++G(d,p)(E)/PCM computational protocols are given in the ESI (Tables S3 and S4†). Interestingly, the σ_{calcd} ^{13}C shielding tensor elements are linearly correlated with the Wiberg Bond Order (WBO) of the Cr–CO$_{trans}$ bond (Fig. S3†) demonstrating that covalent bonding contributions to the Cr–CO$_{trans}$ bond and net charge transfer from ligand L to the Cr metal center are determinants of *trans*-philicity.

Generally no linear correlations exist for the σ_{calcd} ^{13}C *vs.* Cr(4s%), σ_{calcd} ^{13}C *vs.* Cr(4p%) and σ_{calcd} ^{13}C *vs.* Cr(3d%) correlations of the bonding σ(Cr–CO$_{trans}$) NBO for the complete set of ligands L. The same holds true for the σ_{calcd} ^{13}C *vs.* Q_{Cr}, σ_{calcd} ^{13}C *vs.* Q_C, σ_{calcd} ^{13}C *vs.* Occupation of σ(Cr–CO$_{trans}$) NBOs and σ_{calcd} ^{13}C *vs.* Occupation of σ*(Cr–CO$_{trans}$) NBO correlations. However, good linear relationships can be drawn from similar ligand families (subsets) separately. The ligand families contain ligands which are classified either according to the nature of the donor atom or their electronic effects, *i.e.* strong σ donors, σ donor/π acceptor and σ donor/π donors.

The covalent component of the bonding Cr–CO$_{trans}$ natural bond orbital is constructed from an optimum 4s, 4p and 3d orbital population ($s^xp^yd^z$ hybridized orbitals) of the central Cr atom in order to maximize the quantity $S^2/\Delta E$ (S is the overlap integral between metal and ligand orbitals and ΔE is the absolute energy separation between them). The 4s(%), 4p(%) and 3d(%) characters of the $s^xp^yd^z$ hybridized orbitals (being practically sp^3d^2 hybrids) of the Cr metal center used in the bonding σ(Cr–CO$_{trans}$) NBOs are given in the ESI (Table S5†). Indeed good linear relationships between the σ_{calcd} ^{13}C *vs.* Cr(4s%), σ_{calcd} ^{13}C *vs.* Cr(4p%) and σ_{calcd} ^{13}C *vs.* Cr(3d%) correlations are obtained for similar families (subsets) of ligands separately (Fig. S4†).

The linear relationships given in Fig. S4† show an upfield (shielding) shift of σ_{calcd} ^{13}C NMR upon increasing the Cr

(4s%) and Cr(3d%) character of the σ(Cr–CO_{trans}) NBO, but a downfield (deshielding) shift of σ_{calcd} ^{13}C NMR upon increasing the Cr(4p%) character of the σ(Cr–CO_{trans}) NBO.

Plots of the σ_{calcd} ^{13}C *vs.* Q_{Cr} and σ_{calcd} ^{13}C *vs.* Q_C correlations (where Q_{Cr} and Q_C are the natural atomic charges on the Cr and C atom of the CO_{trans} ligand) for $[Cr(CO)_5L]^{-/0/+}$ complexes given in the ESI (Fig. S5†) show also good linear relationships for similar families of ligands separately. It can be seen that the increase of the electron density on the Cr central atom induces an upfield (shielding) shift of the σ_{calcd} ^{13}C shielding tensor elements, while the increase of the positive natural atomic charge on the C atom, that means the decrease of electron density induces, as expected, a downfield (deshielding) shift of the σ_{calcd} ^{13}C shielding tensor elements.

Finally, good linear relationships for the σ_{calcd} ^{13}C *vs.* Occupation of σ(Cr–CO_{trans}) NBOs and σ_{calcd} ^{13}C *vs.* Occupation of σ^*(Cr–CO_{trans}) NBO correlations are also obtained for similar ligand families separately (Fig. S6†). All linear relationships show an upfield (shielding) shift of the σ_{calcd} ^{13}C shielding tensor elements upon increasing the occupation of the σ(Cr–CO_{trans}) NBO and the occupation of the antibonding σ^*(Cr–CO_{trans}) NBOs, due to accumulation of electron density near the C atom of the CO_{trans} ligand.

In summary it can be concluded that the synergy of the σ- and π-covalent bonding contributions to the Cr–CO_{trans} bond and the electron density transfer from L to Cr metal center manipulate *trans*-philicity (*trans*-effect/*trans*-influence) in octahedral $[Cr(CO)_5(L)]^{-/0/+}$ (50 ligands) complexes.

Conclusions

Having analyzed a great deal of computational NMR data (using ^{13}C NMR probe) it is tempting to propose a quantitative *trans*-philicity ladder for a broad series of ligands (50 ligands) for octahedral $[Cr(CO)_5L]^{+/0/-}$ complexes. The NMR *trans*-philicity ladder has been quantified by the calculated $\Delta\sigma = \sigma_{Cr(CO)_5L} - \sigma_{Cr(CO)_5}$ *trans*-philicity descriptor. The *trans*-philicity for ligand L is defined as the strength of philicity of the coordination site in *trans*-position to itself. We also showed that it is possible to retrieve the *trans*-effect and *trans*-influence series of the ligands under study employing the ^{13}C NMR probe. Along this line merging the *trans*-effect and *trans*-influence terms in a unified *trans*-philicity concept avoids confusion in the ambiguous use either of the *trans*-effect or the *trans*-influence terms to describe the same phenomenon, often encountered in coordination chemistry. Important results are summarized as follows:

1. The well established ligand electronic parameters P_L and E_L(L) and other popular electronic/structural descriptors related to the L–Cr–CO_{trans} bonding mode underpin the new concept of *trans*-philicity (*trans*-influence and *trans*-effect) in octahedral coordination and organometallic compounds.

2. A quantitative NMR *trans*-philicity ladder has been built for a broad series of ligands in octahedral $Cr(CO)_5L$ complexes by using a ^{13}C NMR probe. The $\Delta\sigma = \sigma_{Cr(CO)_5L} - \sigma_{Cr(CO)_5}$ NMR parameter, calculated by DFT computational protocols, was used as a sensitive descriptor of *trans*-philicity. The *trans*-philicity ladder goes parallel to the *trans*-effect and *trans*-influence ladders built by the R(Cr–CO_{trans}) and ν(Cr–CO_{trans}) descriptors.

3. Strong π-acceptor ligands exert the strongest *trans*-philicity, while the strong σ-donor ligands exert the weakest *trans*-philicity. Other commonly used ligands in coordination and organometallic chemistry, such as carbenes, pyridine, NH_3, nitriles and phosphanes, exhibit moderate *trans*-philicity.

4. Excellent linear relationships between the isotropic σ ^{13}C shielding tensor elements and the well established ligand electronic parameters P_L and E_L(L) and other popular electronic/structural descriptors related to the L–Cr–CO_{trans} bonding scrutinized the underlying principles and the origin of *trans*-philicity and threw some light on the still intriguing physics of the *trans*-effect.

5. The linear σ_{calcd} ^{13}C *vs.* WBO(Cr–C), σ_{calcd} ^{13}C *vs.* occupancy of bonding σ(Cr–CO_{trans}) and antibonding σ^*(Cr–CO_{trans}) natural bond orbitals, σ_{calcd} ^{13}C *vs.* Q_{Cr} and σ_{calcd} ^{13}C *vs.* Q_C demonstrated that covalent bonding contributions to the Cr–CO_{trans} bond and net charge transfer from ligand L to the Cr metal center are determinants of *trans*-philicity.

6. The strength of the Cr–CO_{trans} bond primarily depends on the Cr(4s%), Cr(4p%) and Cr(3d%) character of the $s^x p^y d^z$ (practically sp^3d^2 type) hybridized orbitals of the Cr metal center used in the formation of the bonding σ(Cr–CO_{trans}) NBO.

Our most important conclusion is that synergic contribution of the σ- and π-covalent bonding to the Cr–CO_{trans} bond and the electron density transfer from L to the Cr metal center manipulate *trans*-philicity in octahedral $[Cr(CO)_5(L)]^{-/0/+}$ complexes.

Conflicts of interest

There are no conflicts to declare.

Notes and references

1 A. Pidcock, R. E. Richards and L. M. Venanzi, *J. Chem. Soc. A*, 1966, 1707–1710.
2 F. Basolo and R. G. Pearson, *Prog. Inorg. Chem.*, 1962, **4**, 381–453.
3 B. J. Coe and S. J. Glenwright, *Coord. Chem. Rev.*, 2000, **203**, 5–80.
4 G. Butler, J. Chatt, G. J. Leigh and C. J. Pickett, *J. Chem. Soc., Dalton Trans.*, 1979, 113–116.
5 J. Chatt, C. T. Kan, G. J. Leigh, C. J. Pickett and D. R. Stanley, *J. Chem. Soc., Dalton Trans.*, 1980, 2032–2038.
6 J. Chatt, Ligand Effects, *Coord. Chem. Rev.*, 1982, **43**, 337–347.
7 A. B. P. Lever, *Inorg. Chem.*, 1990, **29**, 1271–1285.

8 A. B. P. Lever, *Ligand Electrochemical Parameters and Electrochemical-Optical Relationships. Comprehensive Coordination Chemistry II*, Elsevier Pergamon, Amsterdam, The Netherlands, 2005, vol. 2, pp. 251–268.
9 C. A. Tolman, *J. Am. Chem. Soc.*, 1970, **92**, 2953–2956.
10 C. J. Pickett and D. Pletcher, *J. Organomet. Chem.*, 1975, **102**, 327–333.
11 C. A. Tolman, *Chem. Rev.*, 1977, **77**, 313.
12 L. Perrin, E. Clot, O. Eisenstein, J. Loch and R. H. Crabtree, *Inorg. Chem.*, 2001, **40**, 5806–5811.
13 F. Zobi, *Inorg. Chem.*, 2010, **49**, 10370–10377.
14 D. Cremer and E. Kraka, *Dalton Trans.*, 2017, **46**, 8323–8338.
15 T. G. Appleton, C. Clark and L.-E. Manzer, *Coord. Chem. Rev.*, 1973, **10**, 335–422.
16 A. A. Grinberg, *An Introduction to the Chemistry of Complex Compounds*, Pergamon Press, Oxford, 1962.
17 F. R. Hartley, The cis- and trans-Effects of Ligands, *Chem. Soc. Rev.*, 1973, **2**, 163–179.
18 M. J. Wovkulich and J. D. A. Atwood, *Organometallics*, 1982, **1**, 1316–1321.
19 R. F. See and D. Kozina, *J. Coord. Chem.*, 2013, **66**, 490–500.
20 F. Guégan, V. Tognetti, L. Joubert, H. Chermette, D. Luneaub and C. Morell, *Phys. Chem. Chem. Phys.*, 2016, **18**, 982–990.
21 C. Morell, A. Grand and A. Toro-Labbé, *J. Phys. Chem. A*, 2005, **109**, 205–212.
22 P. Geerlings and F. De Proft, *Phys. Chem. Chem. Phys.*, 2008, **10**, 3028–3042.
23 J. I. Martinez-Arraya, *J. Math. Chem.*, 2015, **53**, 451–465.
24 M. Mitoraj and A. Michalak, *J. Mol. Model.*, 2007, **13**, 347–355.
25 A. Michalak, M. Mitoraj and T. Ziegler, *J. Phys. Chem. A*, 2008, **112**, 1933–1939.
26 M. P. Mitoraj, M. Parafiniuk, M. Srebro, M. Handzlik, A. Buczek and A. Michalak, *J. Mol. Model.*, 2011, **17**, 2337–2352.
27 M. J. Frisch, G. W. Trucks, H. B. Schlegel, G. E. Scuseria, M. A. Robb, J. R. Cheeseman, G. Scalmani, V. Barone, B. Mennucci, G. A. Petersson, H. Nakatsuji, M. Caricato, X. Li, H. P. Hratchian, A. F. Izmaylov, J. Bloino, G. Zheng, J. L. Sonnenberg, M. Hada, M. Ehara, K. Toyota, R. Fukuda, J. Hasegawa, M. Ishida, T. Nakajima, Y. Honda, O. Kitao, H. Nakai, T. Vreven, J. A. Montgomery, J. Peralta, J. E. Peralta, F. Ogliaro, M. Bearpark, J. J. Heyd, E. Brothers, K. N. Kudin, V. N. Staroverov, T. Keith, R. Kobayashi, J. Normand, K. Raghavachari, A. Rendell, J. C. Burant, S. S. Iyengar, J. Tomasi, M. Cossi, N. Rega, J. M. Millam, M. Klene, J. E. Knox, J. B. Cross, V. Bakken, C. Adamo, J. Jaramillo, R. Gomperts, R. E. Stratmann, O. Yazyev, A. J. Austin, R. Cammi, C. Pomelli, J. W. Ochterski, R. L. Martin, K. Morokuma, V. G. Zakrzewski, G. A. Voth, P. Salvador, J. J. Dannenberg, S. Dapprich, A. D. Daniels, O. Farkas, J. B. Foresman, J. V. Ortiz, J. Cioslowski and D. J. Fox, 2010.
28 J. P. Perdew, K. Burke and M. Ernzerhof, *Phys. Rev. Lett.*, 1996, **77**, 3865.
29 M. Ernzerhof and G. Scuseria, *J. Chem. Phys.*, 1999, **110**, 5029.
30 C. Adamo and V. Barone, *J. Chem. Phys.*, 1999, **110**, 6158.
31 F. Weigend and R. Ahlrichs, *Phys. Chem. Chem. Phys.*, 2005, **7**, 3297–3305.
32 J. Tomasi, B. Mennucci and R. Cammi, *Chem. Rev.*, 2005, **105**, 2999–3093.
33 A. E. Reed, L. A. Curtiss and F. Weinhold, *Chem. Rev.*, 1988, **88**, 899.
34 F. Weinhold, in *The Encyclopedia of Computational Chemistry*, ed. P. v. R. Schleyer, John Wiley & Sons, Chichester, U.K., 1998.
35 R. Ditchfield, *Mol. Phys.*, 1974, **27**, 789–807.
36 J. Gauss, *J. Chem. Phys.*, 1993, **99**, 3629–3643.
37 J. M. Gleeson and R. W. Vaughan, *J. Chem. Phys.*, 1983, **78**, 5384–5362.
38 *Comprehensive Coordination Chemistry*, ed. G. Wilkinson, R. D. Gillard and J. A. McCleverty, Pergamon Press, Oxford, 1987, vol. I.
39 D.G. Gusev, *Organometallics*, 2009, **28**, 6458–6461.
40 B. Pinter, V. Van Speybroeck, M. Waroquier, P. Geerlings and F. De Proft, *Phys. Chem. Chem. Phys.*, 2013, **15**, 17354.